



Short communication

Mechanical properties of ultra-high pressure sintered sphene (CaTiSiO₅)

Eranezhuth Wasan Awin¹, Branko Matović², Jelena Maletaškić², Vladimir Urbanovich³, Ravi Kumar^{1,*}

¹Materials Processing Section, Department of Metallurgical and Materials Engineering, Indian Institute of Technology-Madras (IIT Madras), Chennai 600036, India

²Institute of Nuclear Sciences Vinca, Department of Materials Sciences, University of Belgrade, Serbia

³Scientific-Practical and Materials Research Center, NAS of Belarus, 19 P. Brovka Street, 220072 Minsk, Belarus

Received 6 June 2016; Received in revised form 1 October 2016; Accepted 8 November 2016

Abstract

The investigation of nano-mechanical properties of sphene sintered under ultra-high pressures in the order of 4 GPa is done using indentation techniques. An indentation hardness of 6.6 GPa and reduced elastic modulus of 112.3 GPa is reported at maximum load of 7 mN. The material exhibits a high elastic recovery (~59.1%) and the nature of deformation mechanism has been comprehended from the plastic work ratio. In addition, the fracture toughness of the material is also evaluated using indentation crack length method.

Keywords: mechanical properties, indentation, hardness, sintering

I. Introduction

Sphene (CaTiSiO₅), a complex orthosilicate mineral, finds its use predominantly in radioactive waste immobilization [1]. The leaching studies performed on glass ceramic based CaSiTiO₅ in an underground vault environment at the depth of 500–1000 m illustrated the excellent durability of this material under these conditions [2]. Apart from being considered as a host material for radioactive nuclear waste, the material also finds use in the field of biomedical engineering. Earlier studies done to improve the osseointegration of Ti-6Al-4V with coatings such as hydroxyapatite (HAP) and calcium silicate (CaSiO₃) have met with limited success due to their reduced integration into the bone. The limitations of these coatings include slow rate of osseointegration and poor mechanical affixation. In recent years, coating of sphene on Ti-6Al-4V seems to have shown immense potential with respect to chemical stability in addition to adhesion strength due to their similar thermal expansion

coefficients in contrast to HAP and CaSiO₃ coatings [3]. Research involving sphene/titania coatings started a decade ago and in one of the recent findings it was exemplified that the heat-treated sphene/titania coatings exhibited enhanced mechanical and corrosion resistance [4]. Recently, Pantic *et al.* [5] performed the synthesis and characterization of sphene sintered under the high pressure (4 GPa) and temperature (1200 °C). The sample sintered at 1200 °C and at pressures in the order of 4.0 GPa showed the highest density. The microstructural characterization of the material revealed highly dense structure with no porosity. The Rietveld refinement and spectroscopic studies indicated structural phase transition from $P2_1/a$ to $A2/a$. The investigation, however, was limited to structural characterization.

In this study, the mechanical stability of sphene sintered by means of high pressure synthesis (HPS) process was investigated via indentation studies. The properties such as hardness, elastic modulus, plastic work ratio as well as the fracture toughness were determined. To the best of our knowledge, these results have not been reported for HPS sphene elsewhere.

*Corresponding author: tel: +91 44 2257 4777, fax: +91 44 2257 4777, e-mail: nvrk@iitm.ac.in

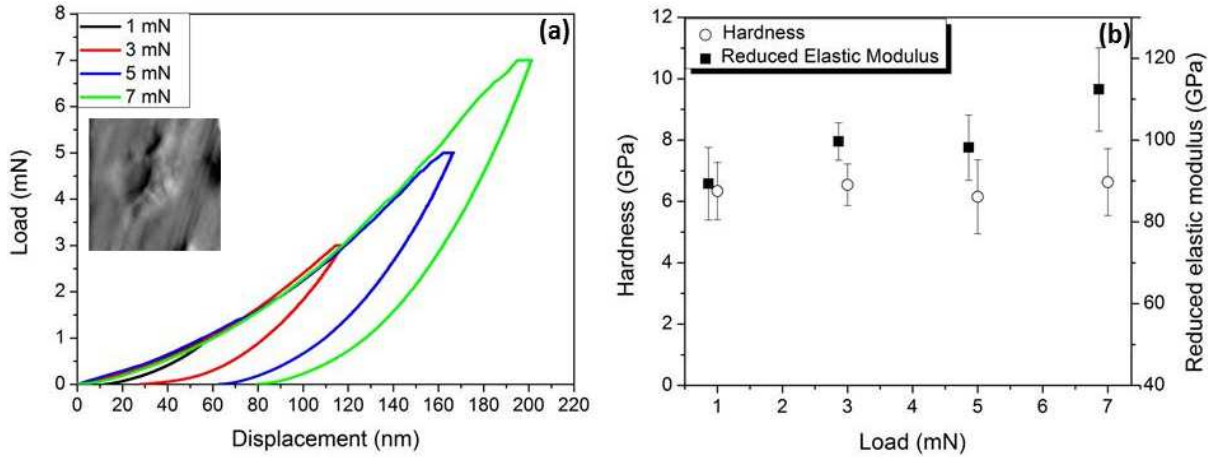


Figure 1. Representative load-displacement curves (inset: SPM image of an indent; image size: 5×5 μm) (a) and reduced elastic modulus with respect to load (b)

II. Experimental

Samples sintered at temperature of 1200 °C and under pressures of 4.0 ± 0.2 GPa using a Bridgman high pressure apparatus were considered for investigation. The processing details on the high pressure synthesis (HPS) of the material can be found elsewhere [5].

Nanoindentation was performed using a Berkovich indenter and the loads were varied between 1 to 7 mN. The loading, holding and unloading time was set to 10 seconds for all the experiments. The area function calibration (25 indents) was done on standard fused quartz silica. The Oliver-Pharr method was used to calculate the hardness (H) and reduced elastic modulus (E_r) from an average value of 10 indents [6]. The scanning probe microscope was used to capture the indent images. The fracture toughness (K_{IC}) calculation was based on the formulation of Anstis [7].

III. Results and discussion

Figure 1a shows representative curves of displacement as a function of load as obtained from the nanoindentation experiments with a maximum penetration depth of ~200 nm at 7 mN. The H and E_r were derived from the following equations:

$$H = \frac{P_{max}}{A} \quad (1)$$

where, P_{max} is the maximum load applied and A is the area function of the indenter.

The E_r can be related to the sample elastic modulus via:

$$\frac{1}{E_r} = \frac{1 - \nu^2}{E} + \frac{1 - \nu_i^2}{E_i} \quad (2)$$

where, E and E_i are the elastic moduli of the sample and diamond Berkovich indenter respectively and ν and ν_i are their respective Poisson's ratio. E_i , ν and ν_i are taken as 1140 GPa, 0.07 and 0.25 respectively. The K_{IC}

was calculated using Anstis equation (3):

$$K_{IC} = 0.016 \left(\frac{E_r}{H} \right)^{0.5} \left(\frac{P}{c^{1.5}} \right) \quad (3)$$

where, P is the load applied in the Vickers hardness test (3 kg) and c is the radius of the critical crack.

The variation of H and E_r with respect to indentation load is exemplified in Fig. 1b. The load had negligible effect on the nanohardness (H) values whereas the elastic modulus (E_r) increased moderately with increase in load. At a peak load of 7 mN, the material displayed H and E of 6.6 and 112.3 GPa, respectively. It was interesting to observe that the deviation in hardness was minimal (well within the standard deviation) with increase in load from 1 mN to 7 mN. The mechanical properties determined on sphene/titania composite coatings revealed the H and E to be ~5 and 100 GPa, respectively and have been attributed to the increase in H and E due to the formation of titania and sphene [4]. Recently, it has also been reported that high pressure/temperature compaction leads to porosity reduction by particle rearrangement [5]. The enhancement in hardness in the present work could be attributed to the highly dense compact obtained after HPS process.

The elastic recovery (amount of energy released by the material after loading) and plasticity index ($\gamma = W_{pl}/W_t$, where W_{pl} and W_t are the work done during the plastic deformation and the total work done, respectively) are two important parameters which can be determined from the nanoindentation curves. The mechanical properties of biomaterials can be characterized using the above mentioned parameters which relate to the elastic and plastic energies associated with the nanoindentation [8]. The elastic recovery (R) is given by the equation (4) [9]:

$$R = \frac{h_{max} - h_f}{h_{max}} \quad (4)$$

Upon the analysis of the unloading curve, the change in R with indentation load was plotted in Fig. 2a and the

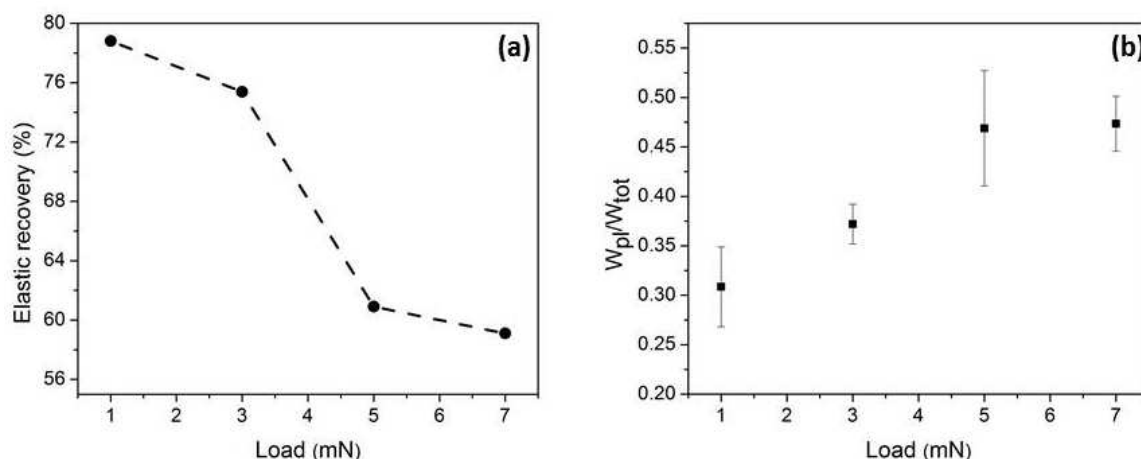


Figure 2. Evolution of elastic recovery (a) and plastic work ratio (b) with indentation load

material showed a high R of $\sim 59.1\%$. The quantitative analysis reported by Pantic *et al.* [10] clearly accounts for 93.3% of sphene, 2.9% of perovskite and 3.8% of coesite for the samples sintered at 1200 °C. The high percentage of sphene as quantified by Reitveld refinement could be accounted for the high elastic recovery. The total work ($W_t = W_e + W_{pl}$) and the elastic work (W_e) done were calculated by accounting the area under the loading and unloading curve respectively. The plastic work done can be eventually deduced from the above equations. Greenwood and Williamson have proposed [11] a model in which it is indicated that if $\gamma > 1$, the material is predominantly plastic whereas if $\gamma < 0.6$, the material is said to deform elastically. The plastic work ratio values obtained in this case (Fig. 2b) suggest that plastic deformation has not been activated even at the maximum load. However at lower loads, the plastic work ratio decreased considerably (0.47–0.31) suggesting the deformation is purely elastic. The materials with high plasticity index are believed to endure high friction which ultimately leads to wear of the components in the long run [12]. Hence the material under investigation could be considered as a suitable replacement from a mechanical perspective for bone implants since the implants are not subjected to noticeable plastic strains.

The HPS sample exhibited a relatively high K_{IC} value of $1.9 \pm 0.2 \text{ MPa}\cdot\text{m}^{1/2}$ in contrast to their counterparts such as HAP ($1 \text{ MPa}\cdot\text{m}^{1/2}$) and CaSiO_3 ($0.5 \pm 0.2 \text{ MPa}\cdot\text{m}^{1/2}$) indicating a possible potential use in biomedical applications [13,14]. Apart from this, the materials with high H/E are said to possess high wear resistance [15] and the HPS sphene with a H/E ratio of around 0.059 is believed to be more wear resistant in contrast to the single crystal HAP ($H = 7 \text{ GPa}$ and $E_r = 143.9 \text{ GPa}$) [16].

IV. Conclusions

The mechanical properties of high pressure compacted sphene were determined using nanoindentation. The material exhibited high hardness, high elastic re-

covery and lower elastic modulus which are characteristic features of materials considered for biomedical applications. The plastic ratio was found to be less than 0.5 suggesting that the material deformed elastically at the maximum load. The fracture toughness value seems promising and material could be an effective replacement for the existing bioactive implant materials.

References

1. P.J. Hayward, E.V. Cecchetto, "Development of sphene-based glass ceramics tailored for Canadian waste disposal conditions", pp. 91–97 in *The Scientific Basis for Nuclear Waste Management*, Ed. S.J. Topp, Elsevier, New York, USA, 1992.
2. P.J. Hayward, F.E. Doern, E.V. Cecchetto, S.L. Mitchell, "Leaching studies of natural and synthetic titanite. A potential host for wastes from the reprocessing of Canadian nuclear fuel", *Can. Mineral.*, **21** (1983) 611–623.
3. C. Wu, Y. Ramaswamy, A. Soeparto, H. Zreiqat, "Incorporation of titanium into calcium silicate improved their chemical stability and biological properties", *J. Biomed. Mater. Res. A*, **86** (2008) 402–410.
4. S. Cheng, W. Daqing, Z. Yu, "Mechanical and corrosion resistance of hydrophilic sphene/titania composite coatings on titanium and deposition and release of cefazolin sodium/chitosan films", *Appl. Surf. Sci.*, **257** (2011) 2657–2664.
5. J. Pantic, V. Urbanovich, V. Poharo-Logar, B. Jokic, M. Stojmenovic, A. Kremenovic, B. Matovic, "Synthesis and characterization of high-pressure and high temperature sphene (CaTiSiO_5)", *Phys. Chem. Miner.*, **41** (2014) 775–782.
6. W.C. Oliver, G.M. Pharr, "An improved technique for determining hardness and elastic modulus using load and displacement sensing indentation experiments", *J. Mater. Res.*, **7** (1992) 1564–1584.
7. G.R. Anstis, P. Chantikul, B.R. Lawn, D.B. Marshall, "A critical evaluation of indentation techniques

- for measuring fracture toughness - I. Direct crack measurements”, *J. Am. Ceram. Soc.*, **64** (1981) 533–538.
8. Y.V. Milman, “Plasticity characteristic obtained by indentation”, *J. Phys. D. Appl. Phys.*, **41** (2008) 1–9.
 9. M.P. Johansson, H. Sjöstrom, L. Hultman, “HREM and nanoindentation studies on BN:C films deposited by reactive sputtering from a B₄C target”, *Vacuum*, **53** (1999) 451–457.
 10. J. Pantic, A. Kremenovic, A. Dosen, M. Prekajski, N. Stankovic, Z. Bascarevic, B. Matovic, “Influence of mechanical activation on sphene based ceramic material synthesis”, *Ceram. Int.*, **39** (2013) 483–488.
 11. J.A. Greenwood, J.B.P. Williamson, “Contact of nominally flat surfaces”, *Proc. R. Soc. Lond. Series. A*, **295** (1966) 300–319.
 12. A. Nakajima, T. Mawatari, “Effects of surface topography and running-in upon rolling contact fatigue life - Evaluation by plasticity index”, *Tribol. Ser.*, **34** (1998) 291–299.
 13. Y.-M. Kong, S. Kim, H.-E. Kim, I.-S. Lee, “Reinforcement of hydroxyapatite bioceramic by addition of ZrO₂ coated with Al₂O₃”, *J. Am. Ceram. Soc.*, **82** (1999) 2963–2968.
 14. Z. Songjue, W. Lianjun, J. Wan, Z. Jianfeng, C. Lidong, “Mechanical properties of CaSiO₃/Ti₃SiC₂ composites and hydroxyapatite forming ability in simulated body”, *Mater. Trans.*, **49** (2008) 2310–2314.
 15. A. Leyland, A. Matthews, “On the significance of the H/E ratio in wear control: a nanocomposite coating approach to optimised tribological behaviour”, *Wear*, **246** (2000) 1–11.
 16. S.S. Saeed, A.G. Karlis, “Micromechanical properties of single crystal hydroxyapatite by nanoindentation”, *Acta. Biomater.*, **5** (2009) 2206–2212.